# Evaluation of GaN:Fe as a High Voltage Photoconductive Semiconductor Switch for Pulsed Power Applications*

**D. Mauch[ξ], J. Dickens[1], V. Kuryatkov[2], V. Meyers[1], R. Ness[3], S. Nikishin[2], and A. Neuber[1]**

[1]*Center for Pulsed Power and Power Electronics, Texas Tech University*
*Lubbock, TX 79409, USA*
[2]*Nanotech Center, Texas Tech University*
*Lubbock, TX 79409, USA*
[3]*Ness Engineering, Inc.*
*San Diego, CA, USA*

## *Abstract*

Semi-insulating Gallium Nitride is evaluated as a candidate material for use as a high voltage photoconductive semiconductor switch (PCSS) for pulsed power applications. The GaN:Fe samples used for this investigation were commercially available, bulk, semi-insulating samples measuring 10 mm x 10 mm x 475 µm. Their optical and crystallographic properties were determined utilizing cathodoluminesence, photoluminescence, RHEED, as well as microwave reflection techniques for carrier lifetime studies. Experimental results are presented elucidating the potential of GaN:Fe sustaining high potential differences in both lateral and vertical geometry devices. For instance, electric field hold-off exceeding 100 kV/cm was observed in lateral geometry with mm sized gaps. In addition, a process for the homo-epitaxial growth of GaN:Si was developed in order to facilitate the fabrication of high quality ohmic contacts. Lastly, experimental results evaluating the on-state performance and photo-current efficiency of a GaN:Fe based PCSS are presented.

## I. INTRODUCTION AND BACKGROUND

In virtually all pulsed power applications, there is a need for high voltage, long lifetime, and highly-controllable switches. A photoconductive semiconductor switch (PCSS) is one class of switch that has the potential to enhance pulsed power system capabilities due to its compact geometry, capability of MHz repetition frequencies, inherent optical isolation, and extremely low switching jitter. As is common in semiconductor technology advancement, the material choice has been driven by the availability of high quality semiconductor material and material parameters. That is, early experiments in the 1970s utilized Si; GaAs has been popular since the late 1980s, and recently SiC has received significant attention [1-6]. The material properties of GaN (bandgap: ≈ 3.39 eV, theoretical breakdown field strength: 3.3 MV/cm, electron mobility: 1,000 $cm^2$/Vs, hole mobility: 200 $cm^2$/Vs) make GaN in theory well suited for a high voltage PCSS [7]. Previous investigations attempting to utilize GaN as a high voltage PCSS had found the maturity of GaN growth technology to be insufficient for producing a research grade PCSS. However, significant advancements have been made recently regarding the growth of high-quality, bulk, GaN substrates [8-10]. Therefore, a preliminary investigation was conducted in order to evaluate the present maturity of commercially available bulk GaN and template GaN (GaN on sapphire), and test prototype GaN PCSSs. This investigation consisted of material and electrical tests to evaluate the quality of the procured GaN material, and switching tests to evaluate the performance of prototype devices. Both the bulk GaN samples (10 mm x 10 mm x ≈ 0.45 mm) and template GaN samples (5 cm diameter x 5 µm – GaN thickness) were commercially available grade samples procured from Kyma Technologies.

## II. MATERIAL TESTS

The procured GaN samples were subjected to the following material characterization tests: Scanning Electron Microscope (SEM) imaging, Reflected High Energy Electron Diffraction (RHEED), X-Ray Diffraction (XRD), Cathodoluminescence, optical transmission and reflection, Microwave Photoconductive Decay (µWPCD), and DC high voltage (HV) testing. A detailed review of these techniques is beyond the scope of this paper, detailed descriptions of these characterization techniques can be found in [11].

### *A. SEM Imaging*

Both bulk and template samples were imaged using a SEM. The purpose of this characterization test was to analyze the physical surface quality of the obtained samples. Shown in Fig. 1 is an image obtained from a bulk sample. The bulk sample demonstrated a number of macro, and micro scale defects. In addition, density of defects near the edge of the sample was significantly

[ξ] email: daniel.mauch@ttu.edu
*Work supported by the U.S. Army ARDEC

UNCLASSIFIED DISTRIBUTION STATEMENT A. Approved for public release.
978-1-4799-8403-9/15/$31.00 ©2015 IEEE

higher than the number of defects near the center of the sample. The bulk samples were finished with a chemical-mechanical polish (CMP). The template samples exhibited significantly fewer macro and micro scale defects. The surface of the template sample were left in their as-grown state, and therefore appeared to be rougher at the nano-scale compared to the bulk samples due to the lack of any polishing.

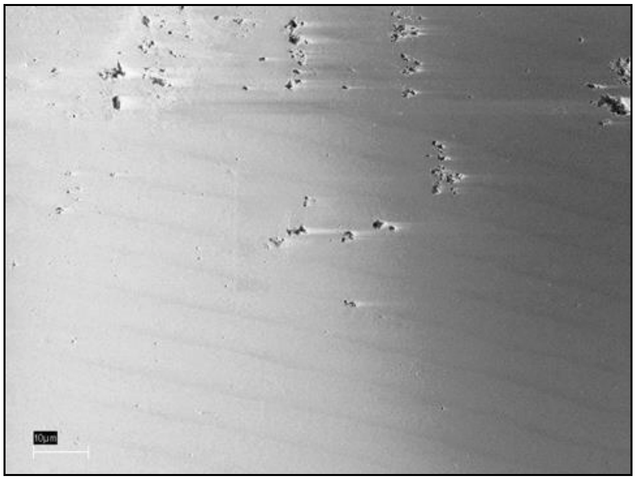

**Figure 1**. SEM image of bulk GaN sample.

### *B. RHEED*

RHEED analysis was conducted on both bulk and template samples. The purpose of this test was to examine the surface composition of the samples. The position of the (00), (01), (-01) reflections along the [11-20] direction of a bulk sample is shown in Fig. 2. The weak reflections are indicative of the presence of a $Ga_2O_3$ oxide layer on the surface of the sample.

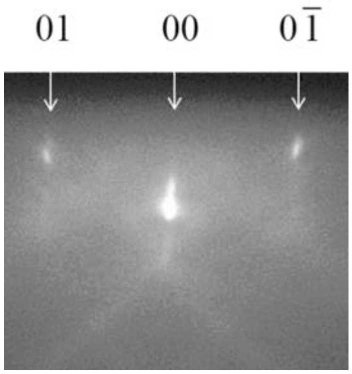


**Figure 2.** RHEED pattern along the [11-20] direction of a bulk GaN sample.

### *C. XRD*

The next characterization test applied was XRD. This test was applied in order to measure the quality of the crystal lattice near the surface of the samples. From these measurements, we were able to estimate the number of edge dislocations being $3x10^7$ $cm^{-2}$ and the number of screw dislocation being $1.6x10^7$ $cm^{-2}$. In addition, data indicative of tensile strain in the GaN crystal lattice was observed and will be detailed elsewhere; this strain is believed to be a consequence of the CMP finish. The (0002) reflection is shown in Fig. 3.

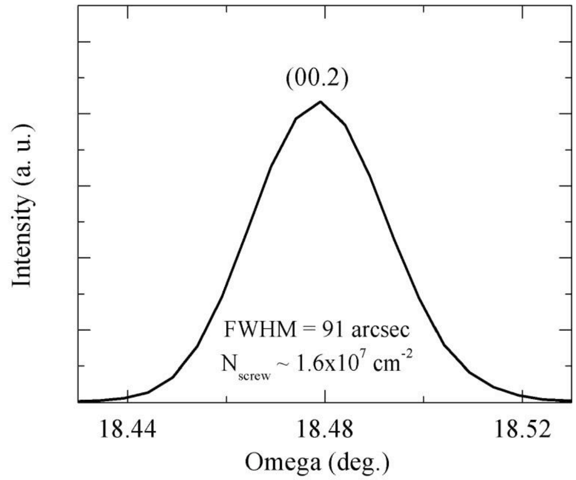


**Figure 3.** XRD scan of the (0002) reflection. The dislocation density was obtained from the peak width.

### *D. Cathodoluminescence*

Cathodoluminescence was also applied to several bulk GaN samples. The two primary peaks observed in the obtained spectra were at 365 nm and 552 nm. These peaks are indicative of the bandgap transition and the iron (Fe) defect. These tests revealed significant variation in the intensity of the Fe peak while the intensity of bandgap transition remained relatively constant. This is attributed to variation of the concentration of the Fe doping from sample to sample. Both samples exhibited a red-shift with increasing beam current while holding the accelerating voltage constant. This is attributed to heating of the sample by the electron beam.

### *E. Optical Transmission and Reflection*

Optical transmission and reflection were applied in order to obtain the wavelength dependent index of refraction and absorption coefficient. The applied method and results are detailed in [12]. This experiment confirmed the band edge position of the absorption spectra at 374 nm.

### *F. µWPCD*

Another applied characterization test was µWPCD. This test was conducted to obtain the effective carrier recombination lifetime. This test was applied to several bulk samples. The recombination lifetime was obtained by numerically fitting the obtained experimental microwave signal. With this technique, recombination lifetimes ranging from 2.0 ns to 5.5 ns were observed.

### *G. DC High Voltage Testing*

The last characterization test applied was DC high voltage testing. In order to implement this test, contact patterns were deposited on several bulk GaN samples. This contact pattern consisted of six electrode pairs ranging in distance from 0.41 mm to 1.17 mm. The metal contacts were deposited with an e-beam evaporator and consisted of Ti/Al/Ni/Au. The IV (current/voltage) of the samples was obtained using a custom HV curve-tracer detailed in [13]. In order to prevent surface-flashover when testing, the samples were either submerged in oil, or encased in an insulating epoxy. The DC HV measurements found significant variation in the HV capability of the procured samples. Some samples were able to effectively block electric fields greater than 100 kV/cm, while other samples were only able to block fields up to 3.5 kV/cm. This variation from sample to sample in their HV capability is believed to be caused by variation in the concentration of the Fe doping.

## III. HOMO-EPITAXIAL GAN:SI GROWTH

Crucial to the production of any high power device is the fabrication of high quality ohmic contacts. Fabricating ohmic contacts to wide-bandgap materials is particularly challenging but is significantly easier if the contacts are made to highly doped material. In addition, a doped sub-contact region reduces the high current densities near the metal-semiconductor interface. Therefore, developing a process for the homo-epitaxial growth of doped GaN on the semi-insulating substrates was essential to fabricating prototype GaN PCSSs. Two MOCVD methods of GaN:Si growth atop the semi-insulating substrates were developed. The first method was based on growth of the GaN:Si layer over the entire substrate surface, followed by removal of the GaN:Si in the necessary regions via plasma etching. The second method achieved selective growth of GaN:Si layer only in the desired regions, thus eliminating the plasma etching step. Both of these methods were able to produce high quality GaN:Si layers up to 700 nm thick atop the semi-insulating substrate with electron concentrations ≈ $3\times10^{18}$ $cm^{-3}$ with a resistivity of ≈ 0.07 Ω-cm. An SEM image of the surface of a selectively MOCVD grown GaN:Si layer is shown in Fig. 4. The wave-like shape of the side wall is a consequence of the mask features; the morphology of the grown layer however was of extremely high quality.

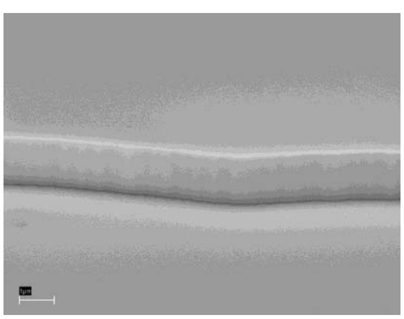

**Figure 4.** SEM image of selectively MOCVD grown GaN:Si contact layer on bulk GaN:Fe

## IV. SWITCHING TESTS

Using the information obtained from the materials characterization tests, several prototype devices were fabricated from both template and bulk substrates. Several template and bulk devices were fabricated and subjected to HV testing. This testing revealed that the majority of the devices were unable to block HV. Subsequently, the best template device and a bulk sample previously used for HV testing were used for switching tests. The circuit diagram of the test circuit used for the switching tests is shown in Fig. 5; the PCSS was triggered with light from a frequency tripled Nd:YAG laser (355 nm, 7 ns FWHM). Typical switching waveforms are shown in Fig. 6.

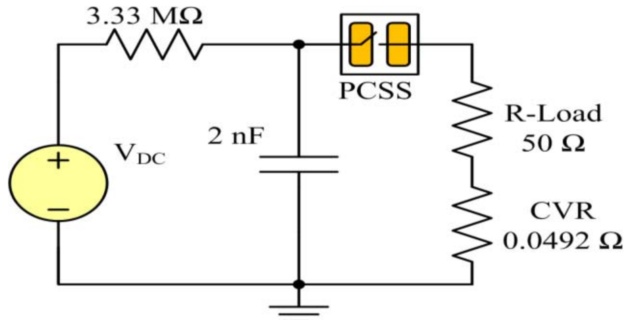


**Figure 5.** Circuit diagram of the test circuit used for testing the prototype PCSSs.

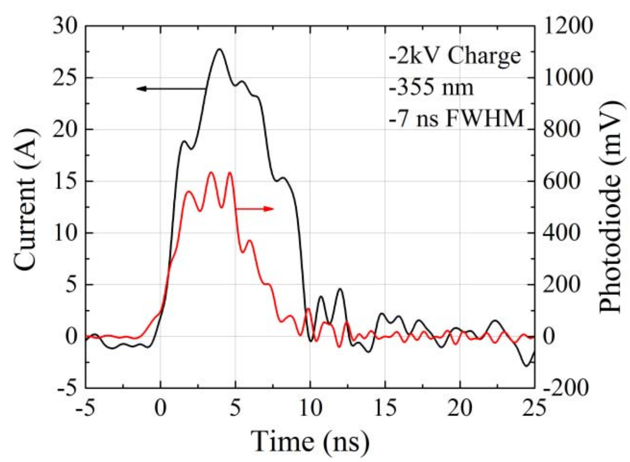


**Figure 6.** Typical switching waveforms for the prototype PCSSs (Black-load current, Red-photodiode signal of the laser pulse).

Both switches were found to effectively function as closing and opening switches. The maximum observed di/dt was 8.25 kA/µs (10/90), and the rise time was 3.03 ns (10/90); both quantities were limited by the rise time of the laser pulse. Both of the PCSSs were evaluated over varying laser energy. The template based device exhibited a minimum resistance of ≈ 35 Ω and the bulk device exhibited a minimum resistance of ≈ 20 Ω. The relatively high on-state resistance is attributed to the thinness of the metal contacts and could be significantly reduced by increasing the thickness of the final Au layer.

## V. CONCLUSION

A preliminary investigation regarding the present state of commercially available GaN material and its suitability for fabricating a HV PCSS was conducted. Various material characterization tests were applied to bulk and template samples. These tests examined the surface quality of the devices, confirmed the presence of a $Ga_2O_3$ layer on the surface of the samples, found the crystal lattice near the surface of the samples to be strained, estimated the defect concentration in the samples to be approximately $4 \times 10^7 cm^{-2}$, revealed indications of significant variation in the Fe doping concentration from sample to sample, and found the effective carrier recombination lifetime to vary between 2.0 ns and 5.5 ns. In addition, significant variation in the HV capability of the samples was observed with one sample exhibiting blocking greater than 100 kV/cm, and another sample only able to sustain fields up to 3.5 kV/cm. Processes were also successfully developed to grow GaN:Si atop the semi-insulating substrates which yielded resistivities of approximately 0.07 Ω-cm. Lastly, switching tests were conducted which found the samples were able to successfully function as closing and opening switches and exhibited a di/dt of 8.25 kA/μs (10/90) and a rise time of 3.03 ns (10/90).

## VI. REFERENCES

[1] D. Auston, “Picosecond optoelectronic switching and gating in silicon,” Applied Physics Letters., vol. 26, no. 3, pp. 101-103, 1975.

[2] F. J. Zutavern, G. M. Loubriel, M. O’Malley, L. Shanwald, W. Helgeson, D. McLaughlin, and B. McKenzie, “Photoconductive semiconductor switch experiments for pulsed power applications,” Electron Devices, IEEE Transactions on, vol. 37, no. 12, pp. 2472-2477, 1990.

[3] J. Sullivan, “High power operation of a nitrogen doped, vanadium compensated, 6H-SiC extrinsic photoconductive switch,” Applied Physics Letters, vol. 104, no. 17, 2014.

[4] K. Kelkar, N. Islam, C. Fessler, and W. Nunnally, “Silicon carbide photoconductive switch for high-power, linear-mode operations through sub-band-gap triggering,” Journal of Applied Physics, vol. 98, no. 9, 2005.

[5] J.-W. Bragg, W. Sullivan III, D. Mauch, A. Neuber, and J. Dickens, “All solid-state high power microwave source with high repetition frequency,” Review of Scientific Instruments, vol. 84, no. 5, 2013.

[6] D. Mauch, W. Sullivan III, A. Bullick, A. Neuber, and J. Dickens, “High Power Lateral Silicon Carbide Photoconductive Semiconductor Switches and Investigation of Degradation Mechanisms," Plasma Science, IEEE Transactions on, vol.43, no.6, pp. 2021-2031, June 2015.

[7] M. E. Levinshtein, S. L. Rumyantsev and M. S. Shur, “Properties of Advanced Semiconductor Materials.” John Wiley & Sons, 2001.

[8] R. Vaudo, X. Xu, C. Loria, A. Salant, J. Flynn, and G. Brandes, “GaN boule growth: A pathway to GaN wafers with improved material quality,” Physica Status Solidi A: Applied Research, vol. 194, no. 2, pp. 494-497, 2002.

[9] D. Hanser, L. Liu, E. Preble, K. Udwary, T. Paskova, and K. Evans, “Fabrication and characterization of native non-polar GaN substrates,” Journal of Crystal Growth, vol. 310, no. 17, pp. 3953-3956, 2008.

[10] H. Amano, “Progress and prospect of the growth of wide-band-gap group III nitrides: Development of the growth method for single-crystal bulk GaN,” Japanese Journal of Applied Physics, vol. 52, no. 5R, 2013.

[11] D. Schroder, “Semiconductor material and device characterization.” John Wiley & Sons, 2006.

[12] V. Meyers, D. Mauch, J. Mankowski, J. Dickens, and A. Neuber, “Characterization of the Optical Properties of GaN:Fe for High Voltage Photoconductive Switch Applications,” Pulsed Power Conference (PPC), 2015 20th IEEE, June 2015.

[13] W. Sullivan III, D. Mauch, A. Bullick, C. Hettler, A. Neuber, and J. Dickens, “ A compact, 45 kV curve tracer with picoampere current measurement capability,” Review of Scientific Instruments, vol. 84, no. 3, 2013.